

Ligand Binding

Helical Propensity in an Intrinsically Disordered Protein Accelerates Ligand Binding**

Vytautas Iešmantavičius, Jakob Dogan, Per Jemth, Kaare Teilum, and Magnus Kjaergaard*

Abstract: Many intrinsically disordered proteins fold upon binding to other macromolecules. The secondary structure present in the well-ordered complex is often formed transiently in the unbound state. The consequence of such transient structure for the binding process is, however, not clear. The activation domain of the activator for thyroid hormone and retinoid receptors (ACTR) is intrinsically disordered and folds upon binding to the nuclear coactivator binding domain (NCBD) of the CREB binding protein. A number of mutants was designed that selectively perturbs the amount of secondary structure in unbound ACTR without interfering with the intermolecular interactions between ACTR and NCBD. Using NMR spectroscopy and fluorescence-monitored stopped-flow kinetic measurements we show that the secondary structure content in helix I of ACTR indeed influences the binding kinetics. The results thus support the notion of preformed secondary structure as an important determinant for molecular recognition in intrinsically disordered proteins.

Intrinsically disordered proteins (IDPs) play important roles in protein interaction networks because of their ability to bind many other proteins and thus to work as signaling hubs. The dynamic nature of living cells means that ligand recognition must be fast, and intrinsic disorder is thus often cited as contributing to rapid molecular recognition.^[1] It is, however, an unresolved controversy whether protein disorder enhances or slows the rate of molecular recognition, and the discussion is largely theoretical because of a lack of good experimental data. Systematic comparisons of binding kinetics reported for disordered and folded systems suggest that IDPs have slightly faster association rates than folded proteins, although conditions that are known to affect binding kinetics such as temperature and ionic strength vary significantly across the interactions compared.^[2] The unbound states often contain transient secondary structure resembling the secondary

structure in complexes with other proteins. This observation has fostered the notion that preformed structural elements speed up binding.^[3] This theory is based on the conformational selection mechanism for molecular recognition, where only a small fraction of folded conformers are binding competent, and increasing this fraction thus enhances the effective association rate. In contrast to this, the fly-casting theory suggests that disordered proteins bind their partners faster than their folded counterparts.^[1a] This kinetic advantage of disorder has been suggested to derive from weak contacts between the disordered protein and the ligand that is subsequently “reeled in” to the folded complex. This gives the protein a greater effective capture radius and increases the chances of binding. It has proven difficult to test these theories experimentally as it is challenging to vary the degree of preformed structure without changing other variables.

In this study, we demonstrate unequivocally that increased helical propensity in an IDP promotes its binding to a protein ligand, although we cannot resolve if the helix is most critical for the initial encounter or for the transition state (TS) for binding. We use the nuclear coactivator binding domain (NCBD) of the CREB binding protein (CBP) and the intrinsically disordered activation domain of ACTR as a model system. Each protein contributes three α -helices to the complex, where ACTR wraps around NCBD making several intermolecular, but few intramolecular tertiary interactions.^[4] In absence of their binding partner, NCBD is mostly folded with a structure resembling that in complex with ACTR,^[5] whereas ACTR is mostly disordered but with transient helix formation, in particular for the N-terminal helix (H1).^[6] The binding between the two domains is rapid and electrostatically steered, and can be followed by stopped-flow fluorimetry.^[7] Hydrophobic contacts mainly form after the rate-limiting transition state as was demonstrated by kinetic Φ -value analysis of mutants removing hydrophobic side chains in the intermolecular interface.^[8] One residue in H1 was a notable exception and was found to be important for the association reaction.^[8] The H1 of ACTR is thus a well-suited system for testing the effect of preformed structure on molecular recognition.

To vary the degree of preformed helicity in H1 of ACTR, we generated a set of helix-modulating mutants. To avoid perturbing intermolecular interactions in the complex, we selected only mutation sites for which all atoms of the side chain are larger than 4 Å away from NCBD in the structure of the complex (PDB:1 KBH).^[4] For these residues, we predicted the bulk helicity of all potential mutations using AGADIR.^[9] To avoid affecting electrostatic interactions and disruption of the hydrogen bonding, mutations that change the charge of the protein or introduce proline residues were

[*] V. Iešmantavičius,^[1] Prof. K. Teilum, Dr. M. Kjaergaard
Department of Biology, University of Copenhagen
Ole Maaløes Vej 5, 2200 København N (Denmark)
E-mail: mk710@cam.ac.uk

Dr. J. Dogan,^[1] Dr. P. Jemth
Department of Medical Biochemistry and Microbiology
Uppsala University
BMC Box 582, 75123 Uppsala (Sweden)

[†] These authors contributed equally to this work.

[**] This work was supported by the Lundbeck Foundation, the Swedish Research Council and a J. C. Jacobsen memorial scholarship from the Carlsberg Foundation. The authors thank Sarah L. Shammas and Joseph M. Rogers for critical comments to the manuscript.

Supporting information for this article is available on the WWW under <http://dx.doi.org/10.1002/anie.201307712>.

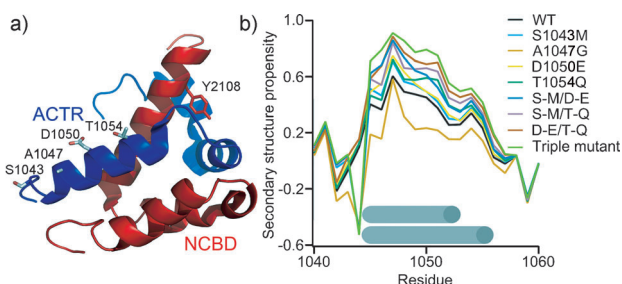


Figure 1. a) Non-interacting mutation sites in ACTR mapped onto the structure of the ACTR:NCBD complex (1KBH). The site of the fluorescent reporter in NCBD (Y2108W) is shown in the stick representation. b) Secondary structure propensity of ACTR variants calculated from ^{13}C chemical shifts show that mutations modulate the preformed helicity in the unbound state of ACTR as predicted. The cylinders illustrate the position of the main helical conformers in the unbound state.

excluded. Four positions were selected for experimental characterization: The three mutants predicted to stabilize the helix the most (S1043M, D1050E, T1054Q) and one mutation predicted to disrupt the helix the most (A1047G; Figure 1). By combining helix-inducing mutants into double and triple mutants, a series of mutants was predicted to have average helical populations of H1 ranging from a few percent to approximately 50%.

We have previously studied the transient secondary structure in this series of mutations using NMR spectroscopy as a method for detecting long-range helix–helix interactions.^[10] In the current study, however, we were interested in quantifying the helical populations under conditions suitable for kinetic measurements. Therefore we re-recorded the backbone chemical shifts of the wild-type and all eight mutants of ACTR at 5°C and under the buffer conditions used for the stopped-flow experiments.^[7] The chemical shift changes (Figure 1b) as well as circular dichroism spectra (Figure S1) showed that all mutations affected the helicity roughly as predicted by AGADIR. To correlate changes in the helical populations with changes in the binding kinetics, the average helical population for each of the nine mutants was determined using ^{13}C chemical shifts based on the secondary structure propensity algorithm.^[11] Appropriate random coil chemical shifts are important to obtain reliable secondary structure propensities from NMR spectroscopy. We thus tried two different sequence-corrected random coil data sets based on either small peptides or databases of chemical shifts.^[12] The secondary chemical shifts and structural propensities were generally very similar for the two random coil datasets (Figure S2), although use of the database-derived chemical shifts proposed by Tamiola et al.^[12c] consistently resulted in a slightly larger helical population. In the following we use the peptide-derived random coil chemical shifts^[12a,b] as these resulted in helical populations in better agreement with previous ensemble simulations.^[10] The two sub-populations with different C-capping residues that were previously detected using residual dipolar couplings,^[10] can be seen in the secondary structure propensity plot as a step towards the C-terminus of the helix. In the following, we use as a measure of the helicity in helix 1 the

average propensity for all residues in the region 1044–1054, which vary from 23% in A1047G to 69% in the S1043M/D1050E/T1054Q triple mutant.

The binding kinetics of the mutants of ACTR were characterized by stopped-flow fluorimetry using a pseudo-wild-type variant of NCBD (Y2108W), in which a tryptophan residue was introduced as a fluorescent probe.^[7] Introduction of the tryptophan residue does not affect the binding kinetics or the stability of the mutant and is thus a valid representative for the wild-type protein.^[7] The observed association rate constant, k_{obs} , was measured as a function of the ACTR concentration (Figure 2a) and the off-rate constant, k_{off} , was measured directly by mixing preformed ACTR:NCBD_{Y2108W} complexes with a large excess of wild-type NCBD (Figure 2b). The second-order rate constant for the association reaction, k_{on} , was extracted from the dependence of k_{obs} on [ACTR] (Figure 2c). k_{on} increases monotonically with increasing helical propensity with a 2.1-fold difference between A1047G and the triple mutant (Figure 2d). Likewise, k_{off} decreases monotonically with increased helical propensity with a 2.5-fold difference between A1047G and

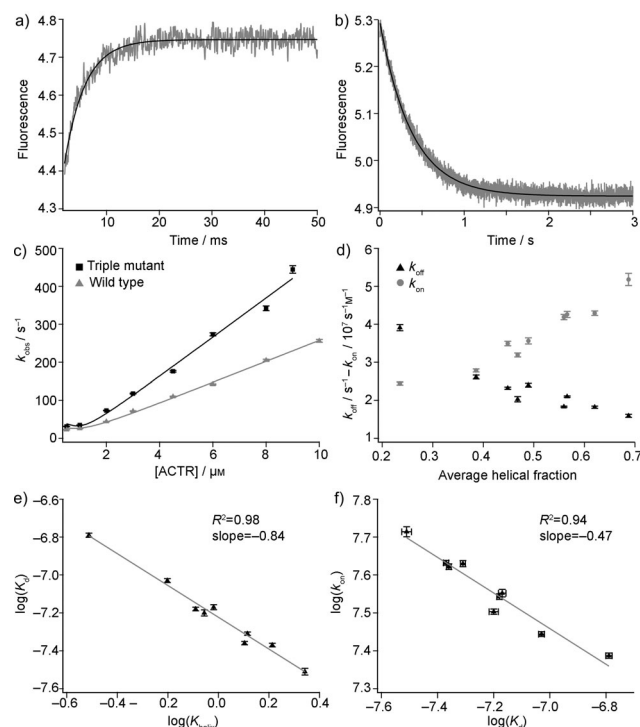


Figure 2. Binding kinetics of ACTR with varying helical propensity to NCBD. a) Kinetic trace for the binding of ACTR_{WT} to NCBD_{Y2108W}. The solid black line is the fit of an exponential decay to the experimental data. b) Kinetic trace for the displacement of NCBD_{Y2108W} in complex with ACTR_{WT} by NCBD_{WT}. The solid line is the fit of an exponential decay to the experimental data. c) The dependence of k_{obs} on ACTR concentration for wild-type and the S1043M/D1050E/T1054Q triple mutant. The solid lines are fits to the general equation for the reversible association of two molecules.^[13] d) Dependence of k_{on} and k_{off} on average helicity in ACTR helix 1. e) Brønsted plot of the affinity of the complex and the equilibrium constant for helix formation. The gray line represents a fit by linear regression of the data. f) Correlation between $\log(k_{\text{on}})$ and $\log(K_{\text{d}})$.

the triple mutant. This dependence of the rate constants on the helicity across a range of mutants suggests that the kinetic effect is indeed an effect of modifying the helical propensity and not unintended modifications of intermolecular interactions or changes to the binding mechanism.

The dissociation constant K_d was obtained from the ratio between k_{off} and k_{on} , which is appropriate for this experimental system.^[8] A Brønsted plot shows a linear correlation (with slope 0.84) between the free-energy of helix formation in the free state, which is proportional to $\log(K_{\text{helix}})$, and the overall free-energy for the binding process, which is proportional to $\log(K_d)$ (Figure 2e). This shows that the helix propensity translates directly into a stabilization of the complex. Similarly, a linear correlation is observed between the free-energy of the transition state for binding, which is proportional to $\log(k_{\text{on}})$, and the overall free-energy for the binding process (Figure 2f). This linear free-energy relation suggests that all helix modifying mutants in ACTR have a similar degree of native interactions formed in the transition state for binding. The slope of the Brønsted plot (-0.47) shows that 47 % of the stabilizing effect of the mutations is based on k_{on} . In a related study, hydrophobic residues from the interface between ACTR and NCBD were systematically investigated by conservative deletion mutations.^[8] The mutations probed mainly tertiary interactions since the predicted effect on helicity is only 3–16 % (see Table S1 in the Supporting Information). On average, 86 % of the destabilizing effect of these mutations was in k_{off} , (average Φ -value = 0.14), thus suggesting that hydrophobic packing occurs mostly after the rate-limiting transition state.^[8] In contrast to this observation, our present results suggest a significant fraction of native helical interactions in the transition state, and thus that formation of helix 1 is more important for the initial events of the binding reaction than native hydrophobic interactions. Similar results were seen for the cMyb-KIX system, in which a high degree of helix formation was observed in the TS for binding-induced folding.^[14] In contrast, low Φ values for helix formation were observed for the S-peptide:S-protein system.^[15]

The usual interpretation of Φ -values is that a value of 0 reflects that the perturbed structure is absent in the TS and a value of 1 reflects that the structure is fully formed. The value of 0.14 for the hydrophobic mutations in the ACTR:NCBD interface suggests that the hydrophobic interactions between ACTR and NCBD are mostly not formed in the TS for binding. It is plausible to interpret the value of 0.47 as H1 in ACTR being 47 % helical in the TS for binding. Increasing the helical propensity thus directly lowers the rate-limiting transition state (Figure 3a). A model that would be able to account for this is a scenario where a rate-limiting folding step occurs after an initial association of a transient complex, and the energy barrier decreases with increased helix propensity (Figure 3a). In this case, it is not the helical population per se, but the helical propensity of the peptide chain that matters. This model resembles the classical induced fit mechanism. In structural terms, this corresponds to a higher success rate for transiently associated complex(es) evolving into the fully formed complex. Intriguingly, this is the opposite of what was found in simulations of the phosphory-

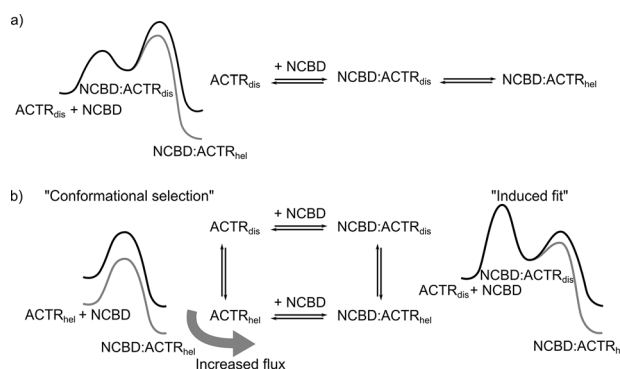


Figure 3. a) Free-energy diagram and kinetic scheme for the binding of ACTR to NCBD via an induced fit mechanism with a rate limiting folding-after-binding step. The gray line represents a mutant with increased helical propensity. b) Free energy diagram and kinetic Scheme for parallel pathways, initiated from either a disordered state, ACTR_{dis} , or a state with preformed H1 helicity, ACTR_{hel} . The increase in k_{on} is caused by a shift in flux to a faster conformational selection pathway (red arrow).

lated kinase-inducible domain (pKID) and the KIX domain of CREB binding protein for which the binding reaction was simulated with a range of preformed helicity.^[2] The association rate increased for more disordered species because they had a higher fraction of binding events resulting in productive binding.^[2] There is, however, no reason to think that every binding reaction should behave identically, as the kinetic effects of helix propensity will depend on the ability of the proteins to make nonnative interactions with the binding partners and the barriers to interconversion between different bound forms.

The fractional slope of the Brønsted plot may also be interpreted as several parallel pathways for formation of the NCBD-ACTR complex.^[16] The simplest such scheme has two pathways: one with H1 in ACTR fully helical and one with it fully disordered (Figure 3b). The two pathways in this model resemble the induced fit and the conformational selection models. Such a model will still result in apparent two-state kinetics if the equilibrium between helix and disorder in ACTR is fast compared to the formation of the complex with NCBD. With the protein concentrations used here the rate of complex formation is below 500 s^{-1} . This is considerably slower than helix formation, which is expected to occur on the nanosecond–microsecond time scale.^[17] In this model, the observed k_{on} and k_{off} values are weighted averages of the rate constants of the two parallel pathways. A mechanism as the suggested with two parallel pathways is expected to result in a nonlinear correlation between $\log(K_d)$ and $\log(k_{\text{on}})$. However, the variation in K_d from 31 nM to 161 nM, corresponding to an interval in $\Delta G_{\text{bind}}^\circ$ of only 3.8 kJ mol^{-1} is too small to identify curvature in the free-energy.^[18] In the absence of changes to the barrier heights of the rate-limiting transition states, an increased helix population will increase the flux of the conformational selection like pathway. Simulations suggest that for the increase in k_{on} to be fully explained by increased flux through the conformational selection pathway, the microscopic association rate constant for this mechanism will have to be approximately ten-fold greater than that of the

induced fit pathway (Figure S3). In this model, the increased rate is due to the increased population of preformed helix that shifts the flux due to mass action. It is inherently difficult to conclusively prove a multi-step mechanism from kinetic data, and it is thus likely that molecular simulations are required to distinguish these two models.

Our data could in principle also experimentally test the fly-casting hypothesis, which predicts that disordered species bind their partners faster due to an increased capture radius. To assess how our mutations affect the capture radius of the protein, we undertook NMR diffusion experiments on wild-type ACTR and the triple mutant (Figure S4). The diffusion coefficient of the triple mutant is essentially identical to that of wild-type ACTR. The compaction caused by the increased helicity is thus insignificant and unlikely to lead to a change in the rate of intermolecular encounters. Fly-casting is thus not likely to contribute significantly to the changes we observe. The proposed effect of the fly-casting effect is relatively small, and may be offset by the slower diffusion of more extended species.^[2a] Any putative fly-casting effect is thus easily masked by a stronger perturbation of other microscopic rate constants as seen in this example.

The experimental data reported here unambiguously demonstrate that helical propensity in ACTR modulates its binding to NCBD, both in terms of association and dissociation, which will provide an optimal experimental benchmark for future computational studies attempting to assign the effect to different microscopic processes. Furthermore, the surprisingly clean data set achieved, suggests that our approach for selecting mutants and our experimental strategy combining NMR spectroscopy and stopped-flow fluorimetry is worth emulating for other systems to determine if the effects of preformed helicity observed here can be generalized to binding of other IDPs.

Experimental Section

Expression and purification of the ACTR and NCBD mutants were described previously.^[7,10] All NMR and stopped flow experiments were performed in 20 mM sodium phosphate, 150 mM NaCl, and pH 7.4 at 277 K. C' and C'' chemical shifts of each ACTR mutant were determined from sets of HNCO, HNCA, and HNCOC spectra recorded on a 750 MHz Varian Inova NMR spectrometer using 0.5 mM protein. The shifts were referenced to DSS (4,4-dimethyl-4-silapentane-1-sulfonic acid).

Binding kinetics were measured on an upgraded Applied Photophysics SX-17MV stopped-flow device. Trp was excited at 280 nm and fluorescence was measured with a 320 nm long-pass filter. Observed rate constants used to deduce k_{on} were measured with $[NCBD_{Y2198W}] = 1 \mu M$ and $[ACTR]$ from 0.5 to 10 μM . Dissociation rate constants were measured by mixing approximately 1 μM preformed $NCBD_{Y2198W}/ACTR$ complex with varying concentrations (up

to 35 μM) of wild-type NCBD. The kinetic data were analyzed as previously described.^[8]

Received: September 2, 2013

Revised: October 28, 2013

Published online: January 21, 2014

Keywords: conformational selection · ligand binding · NMR spectroscopy · proteins · secondary structure

- [1] a) B. A. Shoemaker, J. J. Portman, P. G. Wolynes, *Proc. Natl. Acad. Sci. USA* **2000**, *97*, 8868–8873; b) H. J. Dyson, P. E. Wright, *Curr. Opin. Struct. Biol.* **2002**, *12*, 54–60; c) E. A. Bienkiewicz, J. N. Adkins, K. J. Lumb, *Biochemistry* **2002**, *41*, 752–759; d) P. E. Wright, H. J. Dyson, *Curr. Opin. Struct. Biol.* **2009**, *19*, 31–38; e) G. M. Verkhivker, D. Bouzida, D. K. Gehlhaar, P. A. Rejto, S. T. Freer, P. W. Rose, *Proc. Natl. Acad. Sci. USA* **2003**, *100*, 5148–5153.
- [2] a) Y. Huang, Z. Liu, *J. Mol. Biol.* **2009**, *393*, 1143–1159; b) S. L. Shammass, J. M. Rogers, S. A. Hill, J. Clarke, *Biophys. J.* **2012**, *103*, 2203–2214.
- [3] M. Fuxreiter, I. Simon, P. Friedrich, P. Tompa, *J. Mol. Biol.* **2004**, *338*, 1015–1026.
- [4] S. J. Demarest, M. Martinez-Yamout, J. Chung, H. Chen, W. Xu, H. J. Dyson, R. M. Evans, P. E. Wright, *Nature* **2002**, *415*, 549–553.
- [5] a) M. Kjaergaard, K. Teilum, F. M. Poulsen, *Proc. Natl. Acad. Sci. USA* **2010**, *107*, 12535–12540; b) M. Kjaergaard, F. M. Poulsen, K. Teilum, *Biophys. J.* **2012**, *102*, 1627–1635; c) M. Kjaergaard, L. Andersen, L. D. Nielsen, K. Teilum, *Biochemistry* **2013**, *52*, 1686–1693.
- [6] a) M. Kjaergaard, A.-B. Nørholm, R. Hendus-Altenburger, S. F. Pedersen, F. M. Poulsen, B. B. Kragelund, *Protein Sci.* **2010**, *19*, 1555–1564; b) M.-O. Ebert, S.-H. Bae, H. J. Dyson, P. E. Wright, *Biochemistry* **2008**, *47*, 1299–1308.
- [7] J. Dogan, T. Schmidt, X. Mu, Å. Engström, P. Jemth, *J. Biol. Chem.* **2012**, *287*, 34316–34324.
- [8] J. Dogan, X. Mu, Å. Engström, P. Jemth, *Sci. Rep.* **2013**, *3*, 2076.
- [9] V. Munoz, L. Serrano, *Nat. Struct. Biol.* **1994**, *1*, 399–409.
- [10] V. Išmantavičius, M. R. Jensen, V. Ozenne, M. Blackledge, F. M. Poulsen, M. Kjaergaard, *J. Am. Chem. Soc.* **2013**, *135*, 10155–10163.
- [11] J. A. Marsh, V. K. Singh, Z. Jia, J. D. Forman-Kay, *Protein Sci.* **2006**, *15*, 2795–2804.
- [12] a) M. Kjaergaard, F. M. Poulsen, *J. Biomol. NMR* **2011**, *50*, 157–165; b) M. Kjaergaard, S. Brander, F. M. Poulsen, *J. Biomol. NMR* **2011**, *49*, 139–149; c) K. Tamiola, B. Acar, F. A. A. Mulder, *J. Am. Chem. Soc.* **2010**, *132*, 18000–18003.
- [13] F. Malatesta, *Biophys. Chem.* **2005**, *116*, 251–256.
- [14] R. Giri, A. Morrone, A. Toto, M. Brunori, S. Gianni, *Proc. Natl. Acad. Sci. USA* **2013**, *110*, 14942–14947.
- [15] A. Bachmann, D. Wildemann, F. Praetorius, G. Fischer, T. Kiefhaber, *Proc. Natl. Acad. Sci. USA* **2011**, *108*, 3952–3957.
- [16] a) G. G. Hammes, Y.-C. Chang, T. G. Oas, *Proc. Natl. Acad. Sci. USA* **2009**, *106*, 13737–13741; b) P. Csermely, R. Palotai, R. Nussinov, *Trends Biochem. Sci.* **2010**, *35*, 539–546.
- [17] B. Fierz, A. Reiner, T. Kiefhaber, *Proc. Natl. Acad. Sci. USA* **2009**, *106*, 3–8.
- [18] A. R. Fersht, L. S. Itzhaki, N. F. ElMasry, J. M. Matthews, D. E. Otzen, *Proc. Natl. Acad. Sci. USA* **1994**, *91*, 10426–10429.